Astronomy & Astrophysics manuscript no. Irregulares
December 3, 2014

Astrometric positions for 18 irregular satellites of Giant Planets from 22 years of observations

A. R. Gomes-Júnior[1], M. Assafin[1], R. Vieira-Martins[2], J. I. B. Camargo[2]

[1] Observatório do Valongo/UFRJ, Ladeira Pedro Antônio 43, CEP 20.080-090 Rio de Janeiro - RJ, Brazil
e-mail: altair08@astro.ufrj.br
[2] Observatório Nacional/MCT, R. General José Cristino 77, CEP 20921-400 Rio de Janeiro - RJ, Brazil
e-mail: rvm@on.br

Received ; accepted

ABSTRACT

Context. Context
Aims. Aims
Methods. Methods
Results. Results
Conclusions. Conclusion

Key words. Irregular Satellites

1. Introduction

The Irregular satellites of the giant planets are smaller than the regular ones with more eccentric, inclined, distant and, in most cases, retrograde orbits. Due to its orbital configurations, it's largely accepted that these objects were captured in the early Solar System (Sheppard & Jewitt 2003).

The majority of these objects was discovery in the last decade [1] mainly because they are faint objects. They were never visited by a spacecraft, with the exception of Phoebe, in a flyby by the Cassini space probe in 2004 (Desmars et al. 2013).

There are some hypotheses about the capture methods of objects by Giant Planets. These are the Gas Drag in the primordial circumplanetary nebulae (Sheppard 2006) where the object would be affected by the gas drag and its velocity slowed until being captured by the planet. Another hypotheses is called pull-down capture (Sheppard 2006), where the mass of the planet would increases while the object where temporarily captured.

A hypotheses, based in the Nice model (Morbidelli et al. 2005; Tsiganis et al. 2005; Gomes et al. 2005), was proposed by Nesvorný et al. 2007 and, in the specific case of Jupiter with modern Nice model, by Nesvorný et al. 2014. During the early solar system instability, encounters between the outer planets occurred. These planetary encounters could exchange energy and angular momentum between planets and the objects nearby making it possible for the capture of irregular moons by the giant planets. In this model, the survival rate of prior-LHB satellites is very low.

Another important model is the capture through collisional interactions (Sheppard 2006). A collision between two small bodies in the Hill's sphere of the planet could generate fragmented objects and the dissipated energy could be such a way that some of these objects could be captured.

Some of these objects are in dynamical groups with similar orbital elements, called families, similar to families found in the main belt of asteroids. These families may have been created by a parent body disrupted by collisions with comets or other satellites (Nesvorný et al. 2004). Collisions with comets are more likely to have occurred during the Late Heavy Bombardment (LHB) (Gomes et al. 2005).

Nesvorný et al. 2003 studied the collision rates between irregular satellites and concluded that some satellites could have been removed by collision with a bigger satellite. The rate collision between satellites of the Himalia Group (Himalia, Elara, Lysithea and Leda, mainly), for instance, were found to be more than 1 during the Solar System Age suggesting that their current structure were originated by satellite-satellite collision.

For Phoebe, ejected material from its surface caused by impacts could evolve due to Poynting-Robertson drag and collide with Iapetus causing the large variation in albedo observed on it (Nesvorný et al. 2003). Indeed, Cassini was able to detected in Phoebe an absorption feature at 2.42 μm (probably CN combinations) that was also detected in the dark side of Iapetus (Clark et al. 2005).

If these objects were captured, there remains the question of where do they come from. Clark et al. 2005 showed from imaging spectroscopy from Cassini that Phoebe has a surface probably covered by material from the outer solar system and Grav et al. 2003 showed that the satellites of the Jovian Prograde Group Himalia have grey colors implying that their surfaces are similar to that of C-type asteroids. In this same work, the Jovian Retrograde Group Carme was found to have surface colors similar to the D-type asteroids like Hilda or Trojan families while JXIII Kalyke has a redder color like Centaurs or TNOs.

Send offprint requests to: A. R. Gomes-Júnior
[1] Website: http://ssd.jpl.nasa.gov/?sat_discovery

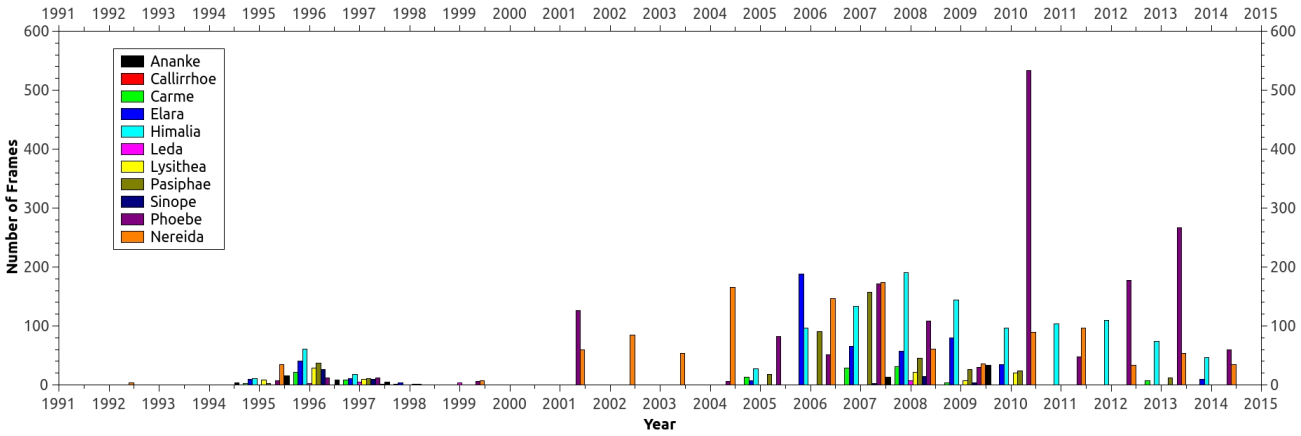

Fig. 1. Distribution of the observations of the satellites over the time from observations at OPD

For Saturnian satellites, Grav & Bauer 2007 showed by their colors and spectral slopes that these satellites contain a more or less equal fraction of C-, P- and D-like objects but SXXII Ijiraq is marginally redder than D-type objects. These works may suggest different origins for the irregular satellites.

In this context, we used 3 databases for deriving precise positions for the irregular satellites observed at Observatório do Pico dos Dias (1.6 m and 0.6 m telescopes, IAU code 874), Observatoire Haute-Provence (1.2m telescope, IAU code 511) and ESO (2.2 m telescope, IAU code 809). More than 100 thousand fits images were obtained between 1992 and 2014 covering a few orbital periods of these objects (12 satellites of Jupiter, 4 of Saturn, Sycorax of Uranus and Nereid of Neptune). These positions will be used in new numerical integrations, generating more precise ephemerides. Stellar occultations by these satellites will be better predicted. Once observed, they will make it possible to obtain the satellites' physical parameters (shape, size, albedo, density) with unprecedented precision.

The observations are described in Sect. 2. The astrometric reductions in Sect. 3. The obtained positions are presented in Sect 4 and analysed in Sect. 5. Conclusions are given in Sect. 6.

2. Observations

Our database consisted in optical images from many observational programs performed with different telescopes/detectors targeting a variety of objects, among which irregular satellites. The observations come from 3 sites: Observatório do Pico dos Dias (OPD), Observatoire Haute-Provence (OHP) and European Southern Observatory (ESO). Altogether there are more than 100 thousand FITS images obtained in a large time span (1992-2014). The instruments and images characteristics are described in the following subsections.

2.1. OPD

The first database was produced at Observatório do Pico dos Dias (OPD, IAU code 874)[2], located at geographical longitude +45° 34′ 57″, latitude −22° 32′ 04″ and an altitude of 1864 m, in Brazil. More than 100 thousand images were observed in 615 nights (244 with Perkin-Elmer, 319 with Boller & Chivens and 52 with Zeiss) between 1992 and 2014 by our group. In Fig 1 there are the quantity of frames obtained by satellite over the time of observations and in Fig 2 the number of frames by satellite for each telescope. Two telescopes of 0.6 m diameter (Zeiss and Boller & Chivens) and one 1.6 m diameter (Perkin-Elmer) were used for the observations.

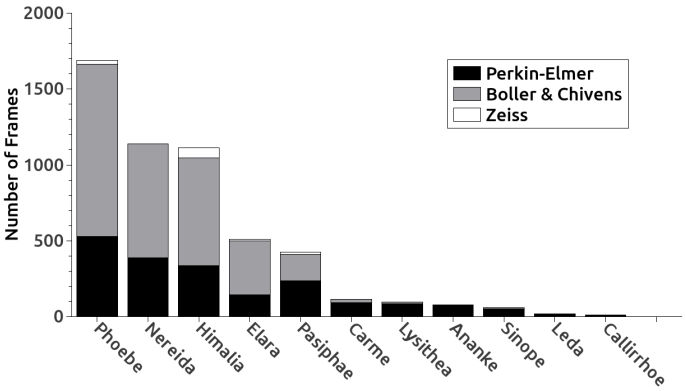

Fig. 2. Number of frames observed by satellite by OPD telescope

This is a inhomogeneous database with observations made with 9 different detectors (see Table 1) and 6 different filters. Many of the oldest images headers had missing coordinates or wrong time and in some cases we couldn't identify the detector. The method used to solve this problem will be given in the Sect. 3.

Table 1. Characteristics of OPD detectors used in this work

Detector	Image Size (pixel)	Pixel Size (μm/px)
CCD048	770 x 1152	22.5
CCD098	2048 x 2048	13.5
CCD101	1024 x 1024	24.0
CCD105	2048 x 2048	13.5
CCD106	1024 x 1024	24.0
CCD301	385 x 578	22.0
CCD523	455 x 512	19.0
IKON	2048 x 2048	13.5
IXON	1024 x 1024	13.5

The plate scale of the telescopes are 13.09"/mm for Perkin-Elmer, 25.09"/mm for Boller & Chivens and 27.5"/mm for Zeiss.

[2] Website: http://www.lna.br/opd/opd.html - in Portuguese

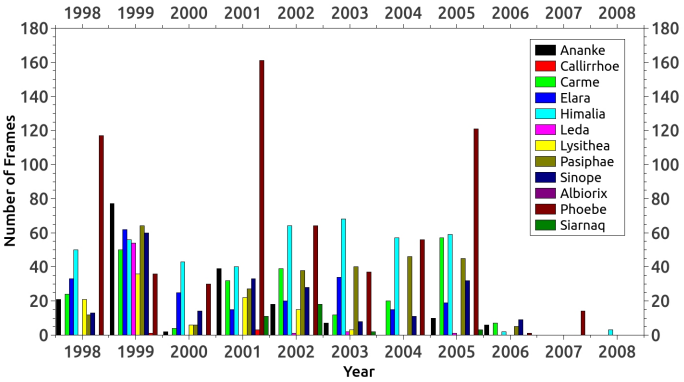

Fig. 3. Distribution of the observations of the satellites over the time from observations at OHP

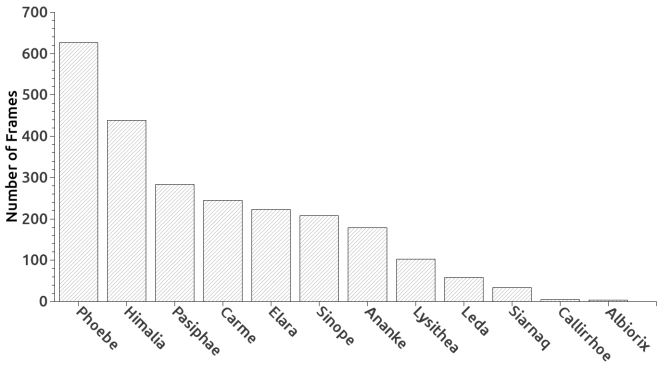

Fig. 4. Number of frames observed by satellite observed at OHP

2.2. OHP

The instrument used at the Observatoire de Haute Provence (OHP, IAU code 511, 5° 42′ 56.5″ E, 43° 55′ 54.7″N, 633.9 m) was the 1.2m-telescope in a Newton configuration. The focal length is 7.2 m. This database contains more than 20 thousand images obtained in 355 nights between 1997 and 2008. During this time only one CCD detector 1024×1024 was used. The size of field is $12' \times 12'$ with a pixel scale of 0.69″. All the images were acquired without the use of filters. Fig. 3 shows the Distribution of the observation of the satellites over the time and Fig. 4 the number of frames observed for each satellite.

2.3. ESO

Observations were made at the 2.2 m Max-Planck ESO (ESO2p2) telescope (IAU code 809) with the Wide Field Imager (WFI) CCD mosaic detector. Each mosaic is composed by eight CCDs of $7.5' \times 15'$ (RA, Dec) size, resulting in a total coverage of $30' \times 30'$ per mosaic. Each CCD has $4k \times 2k$ pixel with a pixel scale of 0.238″. The filter used was a broad-band R filter (ESO#844) with $\lambda_c = 651.725$ nm and $\Delta\lambda = 162.184$ nm. The telescope was shifted between exposures in such a way that each satellite was observed at least twice in different CCDs.

The satellites were observed in 24 nights, divided in 5 missions, between April 2007 and May 2009 during the program that observed stars along the sky path of trans-neptunian objects (TNOs) to identify candidates to stellar occultation as presented in Assafin et al. (2012).

3. Reduction

Almost all the frames were photometrically calibrated with auxiliary bias and flat-field frames by means of standard procedures using IRAF[3] and, for the mosaics, using the esowfi (Jones & Valdes 2000) and mscred (Valdes 1998) packages. Some of the nights at OPD didn't have bias and flat-field images so the correction was not made.

The astrometric reductions were made by the use of the Platform for Reduction of Astronomical Images Automatically (PRAIA) (Assafin et al. 2011). The (x, y) measurements were performed with 2-dimensional circular symmetric Gaussian fits within 1 Full Width Half Maximum (FWHM = seeing). Within 1 FWHM, the image profile is well described by a Gaussian profile, free from the wing distortions, which jeopardize the center determination. PRAIA automatically recognizes catalog stars and determines (α, δ) with a number of models relating the (x, y) measured and (X, Y) standard coordinates projected in the sky tangent plane.

In the OPD database, there were some images, mostly the older ones had missing coordinates or wrong time in their headers. In the case of missing coordinates, we made the reduction many times, each time with the coordinate of a distinct satellite. If the coordinate was nearly correct, PRAIA would manage to identify the field and the satellite if present. When the time wasn't correct, the correction was made only in date, since this information is well registered.

For the ESO images, first the astrometry of the individual CCDs was performed and the (x, y) measurements were corrected by the field distortions patterns determined by Assafin et al. (2012). Finally, all positions coming from different CCds and mosaics were combined to produce a global solution for each night and field observed, and final (α, δ) object positions were obtained in the UCAC4 system.

We used the UCAC4 (Zacharias et al. 2013) as the practical representative of the International Celestial Reference System (ICRS), and the six constants polynomial to model the (x, y) measurements to the (X, Y) tangent plane coordinates. To help identifying the satellites in the frames, and derive the ephemeris for the instants of the observations for comparisons (see Sect 5), we used the kernels from SPICE/JPL[4]. The JPL ephemeris that represented the Jovian satellites was the DE421 + JUP300. For the Saturnian satellites the ephemeris was DE421 + SAT359 to Hyperion, Iapetus and Phoebe and DE421 + SAT361 to Albiorix, Siarnaq and Paaliaq. The DE421 + URA095 was used for Sycorax and DE421 + NEP081 for Nereid.

From Table 2 to 6 there are the mean error in α and δ obtained after these processes by telescope for each satellite. The final number of frames, number of nights and the mean number of UCAC4 stars used in the reduction are also given.

4. Satellite Positions

5. Comparison with current ephemeris

Intending to see the potential of our results to improve the ephemeris of the irregular satellites observed, we analysed the offsets of our positions related to the ephemeris mentioned at Sect. 3. In Fig. 5 there are the mean offsets for

[3] Website: http://iraf.noao.edu/
[4] Website: http://naif.jpl.nasa.gov/naif/toolkit.html

Table 2. Astrometric (α, δ) reduction for each satellite observed with the Perkin-Elmer telescope

Perkin-Elmer					
Satellite	Mean errors σ_α mas	σ_δ mas	Nr frames	Nr nights	UCAC4 stars
Ananke	93.9	185.7	52	7	40
Callirrhoe	66.6	35.4	9	1	3
Carme	97.0	94.3	68	7	49
Elara	230.8	118.7	99	12	32
Himalia	290.5	45.4	238	18	37
Leda	207.4	79.0	6	6	46
Lysithea	107.0	79.4	53	8	41
Pasiphae	157.0	92.5	144	13	22
Sinope	155.0	77.3	37	8	42
Phoebe	73.7	95.3	410	22	6
Nereid	200.3	142.5	289	29	8

Mean errors are the standard deviations in the (O−C) residuals from (α, δ) reductions with the UCAC4 catalog.

Table 3. Astrometric (α, δ) reduction for each satellite observed with the Boller & Chivens telescope

Boller & Chivens					
Satellite	Mean errors σ_α mas	σ_δ mas	Nr frames	Nr nights	UCAC4 stars
Carme	68.5	111.4	22	4	45
Elara	55.4	43.0	294	23	53
Himalia	83.2	43.2	560	31	57
Lysithea	23.6	42.7	7	2	60
Pasiphae	128.5	71.1	140	14	57
Sinope	59.7	17.3	4	1	22
Phoebe	43.8	48.4	810	42	17
Nereid	61.0	45.6	514	38	20

Mean errors are the standard deviations in the (O−C) residuals from (α, δ) reductions with the UCAC4 catalog.

Table 4. Astrometric (α, δ) reduction for each satellite observed with the Zeiss telescope

Zeiss					
Satellite	Mean errors σ_α mas	σ_δ mas	Nr frames	Nr nights	UCAC4 stars
Elara	17.5	21.4	10	1	146
Himalia	112.4	72.3	56	4	91
Pasiphae	24.6	25.1	11	1	140
Phoebe	37.2	30.6	19	1	16

Mean errors are the standard deviations in the (O−C) residuals from (α, δ) reductions with the UCAC4 catalog.

each night and their dispersions plotted by True Anomaly in Right Ascension (5a) and Declination (5b). An overview of the Fig. 5b clearly show us a systematic error in the ephemeris in declination that is when Carme is close to its apojove (True Anomaly = 180°) its offsets are more likely to be more negative than those close to its perijove (True Anomaly = 0°).

For this reason, we conclude there are an error in the inclination of the orbit of Carme. This effect is the most evident and were also observed for others satellites, for instance Ananke and Pasiphae. For some satellites, the orbital coverage is not enough to make a conclusion about their systematic errors in the orbital elements.

Table 5. Astrometric (α, δ) reduction for each satellite observed with the OHP telescope

OHP					
Satellite	Mean errors σ_α mas	σ_δ mas	Nr frames	Nr nights	UCAC4 stars
Ananke	100.6	89.0	141	20	62
Carme	114.9	96.3	204	29	39
Elara	52.0	61.2	187	25	37
Himalia	49.6	66.6	357	43	49
Leda	118.8	33.1	48	7	14
Lysithea	63.0	50.8	84	13	56
Pasiphae	101.0	75.9	248	32	39
Sinope	196.1	73.4	169	25	43
Albiorix	179.0	188.5	4	1	40
Phoebe	30.5	31.9	516	63	51
Siarnaq	46.5	98.4	20	6	32

Mean errors are the standard deviations in the (O−C) residuals from (α, δ) reductions with the UCAC4 catalog.

Table 6. Astrometric (α, δ) reduction for each satellite observed with the ESO telescope

ESO					
Satellite	Mean errors σ_α mas	σ_δ mas	Nr frames	Nr nights	UCAC4 stars
Ananke	225.4	19.1	57	3	761
Callirrhoe	44.6	43.1	20	1	493
Carme	140.4	110.8	37	4	1074
Elara	112.2	87.9	46	4	1492
Himalia	76.7	74.1	23	2	1153
Leda	60.3	125.5	44	3	632
Lysithea	76.4	88.4	90	6	695
Megaclite	52.7	34.9	10	1	445
Pasiphae	70.6	114.8	66	5	836
Praxidike	7.8	38.2	2	1	1934
Sinope	339.1	70.2	11	2	1542
Themisto	894.1	28.5	16	2	1232
Albiorix	76.0	50.9	46	6	330
Paaliaq	301.4	59.0	11	4	382
Phoebe	102.1	57.9	32	5	312
Siarnaq	86.2	66.3	56	6	283
Sycorax	150.7	82.2	35	9	375
Nereid	115.4	78.5	99	12	362

Mean errors are the standard deviations in the (O−C) residuals from (α, δ) reductions with the UCAC4 catalog.

6. Conclusions

We managed to reduce a large database with more than 100 thousand FITS images observed by 5 telescopes in 3 sites between 1992 and 2014 searching for positions of the irregular satellites of the giant planets. We used PRAIA and UCAC4 catalogue to determine the coordinate of all the object in the images and find our targets.

The number of positions found were more than 6000 for 18 satellites (12 of Jupiter, 4 of Saturn, 1 of Uranus and

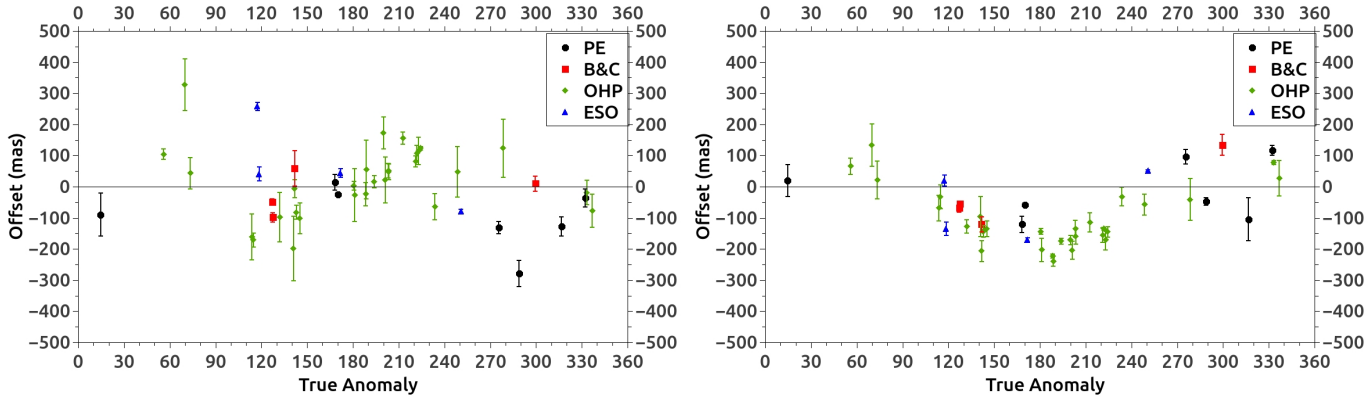

(a) Right Ascension (b) Declination

Fig. 5. Mean Offset and dispersion in the coordinates of Carme taken night by night by True Anomaly

Table 7. Comparison of positions obtained with Jacobson et al. 2012

	Number of Positions				
Satellite	OPD	OHP	ESO	Total	Horizons*
Ananke	52	141	57	250	600
Callirrhoe	9	-	20	29	95
Carme	90	204	37	331	973
Elara	403	187	46	636	1115
Himalia	854	357	23	1234	1757
Leda	6	48	44	98	178
Lysithea	60	84	90	234	431
Megaclite	-	-	10	10	50
Pasiphae	295	248	66	609	1629
Praxidike	-	-	2	2	59
Sinope	41	169	11	221	854
Themisto	-	-	16	16	55
Albiorix	-	4	46	50	137
Paaliaq	-	-	11	11	82
Phoebe	1239	516	32	1787	3479
Siarnaq	-	20	56	76	239
Sycorax	-	-	35	35	237
Nereid	803	-	99	902	716

Comparison between the number of positions obtained in our database with the number used in the numerical integration of Horizons as published by Jacobson et al. 2012.
* Jacobson et al. 2012

1 of Neptune). For some satellites the number is comparable to the number used in the numerical integration of JPL ephemeris (Jacobson et al. 2012) (See Table 7). And systematic errors in the ephemeris were found for some satellites.

Acknowledgements.

References

Assafin, M., Camargo, J. I. B., Vieira Martins, R., et al. 2012, Astronomy and Astrophysics, 541, A142
Assafin, M., Vieira Martins, R., Camargo, J. I. B., et al. 2011, in Gaia follow-up network for the solar system objects : Gaia FUN-SSO workshop proceedings, held at IMCCE -Paris Observatory, France, November 29 - December 1, 2010. ISBN 2-910015-63-7, ed. P. Tanga & W. Thuillot, 85–88
Clark, R. N. et al. 2005, Nature, 435, 66
Desmars, J. et al. 2013, Astronomy and Astrophysics, 553
Gomes, R., Levison, H. F., Tsiganis, K., & Morbidelli, A. 2005, Nature, 435, 466
Grav, T. & Bauer, J. 2007, Icarus, 191, 267
Grav, T., Holman, M. J., Gladman, B. J., & Asknes, K. 2003, Icarus, 166, 33
Jacobson, R. et al. 2012, The Astronomical Journal, 144, 8 pgs
Jones, H. & Valdes, F. 2000, in "Handling ESO WFI Data With IRAF", ESO Document number 2p2-MAN-ESO-22200-00002
Morbidelli, A., Levison, H. F., Tsiganis, K., & Gomes, R. 2005, Nature, 435, 462
Nesvorný, D., Alvarellos, J. L. A., Dones, L., & Harold, L. 2003, The Astronomical Journal, 126, 398
Nesvorný, D., Beaugé, C., & Dones, L. 2004, The Astronomical Journal, 127, 1768
Nesvorný, D., Vokrouhlický, D., & Deienno, R. 2014, The Astronomical Journal, 784, 22
Nesvorný, D., Vokrouhlický, D., & Morbidelly, A. 2007, The Astronomical Journal, 133, 1962
Sheppard, S. S. 2006, in "Outer Irregular Satellites of the Planets and Their Relationship with Asteroids, Comets and Kuiper Belt Objects", IAU Symposium No. 229, 2006, pgs 319-334
Sheppard, S. S. & Jewitt, D. C. 2003, Nature, 423, 261
Tsiganis, K., Gomes, R., Morbidelli, A., & Levison, H. F. 2005, Nature, 435, 459
Valdes, F. G. 1998, in "The IRAF Mosaic Data Reduction Package" in Astronomical Data Analysis Software and Systems VII, A.S.P. Conference Ser., Vol 145, eds R. Albrecht, R. N. Hook and H. A. Bushouse, 53
Zacharias, N., Finch, C. T., Girard, T. M., et al. 2013, AJ, 145, 44